

# Influence of boundary conditions on the dynamics of pattern forming systems: the case of oscillatory media.

S. Bouzat \* and H. S. Wio †

*Grupo de Física Estadística ‡*

*Centro Atómico Bariloche (CNEA) and Instituto Balseiro (CNEA and UNC),  
8400-San Carlos de Bariloche, Argentina*

We study the pattern dynamics in a reaction diffusion model of the activator-inhibitor type in the oscillatory regime. We consider finite systems with partially absorptive boundary conditions analyzing examples in different geometries in one and two dimensions. We observe that the boundary conditions have important effects in the pattern forming properties of the systems. In all the studied cases, the arising complex behaviour is found to be dependent on the absorption parameter. By changing this parameter we can control the asymptotic behaviour to be stationary, periodic, quasiperiodic or chaotic.

## I. INTRODUCTION

There are many properties in pattern forming reaction-diffusion systems that do not depend on the geometry of the system (for instance Turing wavelengths, frequencies of oscillation, shapes and velocities of waves or fronts.) [1]. Due to this fact, most studies on pattern formation have not paid too much attention to features such as the shapes and sizes of the reactors or the boundary conditions, working mainly with infinite systems or periodic boundary conditions. However, it is well known that boundaries and boundary conditions can play a relevant role in determining the behaviour of this kind of systems. For instance, in reference [2] the importance of geometrical characteristics is quite remarkable. Also, recent theoretical papers have shown that the domain shape may have an important effect in the propagation of waves in excitable media [3], and that the consideration of non trivial boundary conditions [4] in some reaction diffusion-systems leads to qualitatively different dynamic behaviour from the one obtained in infinite media.

Here we analyze problems where the boundary conditions (bc's), as well as the size of the system, are relevant parameters determining the kind of complex dynamics arising. We study an activator-inhibitor model in the oscillatory regime considering different geometries with partially absorptive bc's. For a density field  $\rho(\vec{r}, t)$  of a given reactant this condition is written as

$$-D(\nabla\rho)|_{\sigma} \cdot \vec{n} = k\rho|_{\sigma}, \quad (1)$$

where  $D$  is the diffusion constant, the subscript  $\sigma$  indicates evaluation at the boundary,  $\vec{n}$  is the unit vector normal to the boundary in the outer direction, and  $k(\geq 0)$  is the absorption or albedo parameter. This relation expresses the fact that there is an outgoing flux of reactants through the boundary which is proportional to the density. The limit  $k = 0$  corresponds to no flux or Neumann bc's, which means a perfectly reflecting (non absorbing) boundary, whereas clearly, an increasing value of  $k$  corresponds to an increasing absorption at the boundary, and a reduced reflectivity.

We consider the reaction-diffusion model given by the equations

$$\begin{aligned} \dot{u} &= \nabla^2 u + f(u) - v \\ \dot{v} &= D_v \nabla^2 v + u - \gamma v - c, \end{aligned} \quad (2)$$

where the non linear function  $f(u) = -(u - u_0)^3 + u$  characterizes the autocatalytical properties of the activator  $u$ . The model shares the general features of more realistic ones describing chemical systems such as the Belousov Zhabotinskii or CIMA reactions [5,6]. For  $u_0 = c = 0$ , it was used in the analysis of the propagation of fronts in bistable systems [7] and also in the study of pattern formation in inhomogeneous media [8,9]. The constant  $c$  is here set equal to  $[u_0(1 - \gamma)]$ . With this election  $u_0$  represents a translation of the related spatially independent system (i.e. Eqs. (2) without diffusion terms) in the  $(u, v)$ -plane along the line  $(u = v)$ . For  $\gamma > 1$  the equations describe a

---

\*Electronic address: bouzat@cab.cnea.gov.ar; Fellow of CONICET, Argentina

†Electronic address: wio@cab.cnea.gov.ar; Member of CONICET, Argentina

‡http://cab.cnea.gov.ar/cab/invBasica/fisEstad/estadis.htm

bistable medium, while for  $\gamma < 1$  they describe an oscillatory one. Here, we consider  $\gamma = .9$ . In order to work with positive values of the densities  $u$  and  $v$ , we set  $u_0 = .4$ . This last fact is desirable taking into account the kind of bc's we will work with, however, it is not strictly necessary, as we have found the same kind of results (in all the problems here discussed) using  $u_0 = 0$ .

For the chosen values of parameters, the homogeneous system associated to Eqs. (2) has a limit cycle solution of period  $\tau_0 \simeq 14.66$ . As initial conditions for our extended system we consider homogeneous states belonging to this limit cycle. This (natural) choice is taken in order to focus our attention on the effects caused by the boundary conditions. The consideration of inhomogeneous initial states would produce additional pattern forming phenomena that would interact with those coming from the boundary conditions. An important characteristic of the extended system is that, for  $D_v > 1,73$ , a Turing instability [1,10] of wavelength  $\lambda_T \simeq 13$  coexists (and competes) with the Hopf instability [1,10].

The aim of this paper is to show that a wide spectrum of possibilities concerning pattern dynamics arises when different boundary conditions are considered in an oscillatory medium. We would like to attract the interest of experimentalists to study these situations. The experimental observation of the phenomena here predicted might be realized by adequately designing chemical systems sharing the properties of our models. Also, the partially absorptive conditions may appear in real systems as defects at the boundaries, such as, small separations between the gel and the wall of the reactor containing the solution with uncontrolled concentration of reactants. Another experimental possibility is to work with electrical systems [11].

All numerical calculations were done as follows. Firstly, the different systems of partial differential equations have been approximated by systems of coupled ordinary differential equations, obtained by finite difference schemes. Secondly the resulting equations have been solved by a Runge–Kutta 2 method. Different space and time discretization schemes were employed in order to check the results.

The organization of the paper is as follows: in Section II we study a unidimensional system with Neumann boundary conditions at one border and partially absorptive at the other. In Section III we study two different bidimensional systems corresponding to a circular reactor with partially absorptive boundary conditions and a long rectangular system with different boundary conditions on its walls. The last Section is devoted to discussing the results and drawing some conclusions.

## II. UNIDIMENSIONAL SYSTEM.

We now consider Eqs.(2) in the one dimensional domain  $0 \leq x \leq L$ , with Neumann bc's at  $x = 0$  and partially absorptive bc's at  $x = L$ :

$$\begin{aligned} \partial_x u(0) &= 0 & D_v \partial_x v(0) &= 0 \\ \partial_x u(L) &= -k_u u(L) & D_v \partial_x v(L) &= -k_v v(L). \end{aligned} \tag{3}$$

As initial conditions we consider homogeneous states belonging to the limit cycle of the associated non extended system (Eqs. (2) without diffusion). We analyze the dynamics for different values of  $L, D_v, k_u$  and  $k_v$ .

At short times, near  $x = 0$ , where there are Neumann bc's, the system evolves very close to the natural homogeneous limit cycle of the medium; whereas, near  $x = L$ , the motion is perturbed by the albedo bc's which cause the local oscillations to be slower and of smaller amplitude. This effect increases with the absorption parameter. Hence, the dynamics of the system begins to be inhomogeneous and the perturbation is transmitted from  $x = L$  to the rest of the system, which asymptotically reaches different dynamical regimes depending on the parameters. The resulting regime is independent of the initial condition (when taken on the limit cycle as mentioned above) except maybe in some specific parameter regions, as we will discuss later.

For very high absorption, the oscillations near  $x = L$  are inhibited. As a consequence of this, for small enough systems (typically  $L < 2\lambda_T$ , but depending on  $D_v$  and  $k$ 's), the oscillations are found to be stopped in the whole system and stationary patterns are generated. This is because the stationary tendency of the zone near  $x = L$  affects the whole system. The effect is increased when  $D_v$  grows, since the coupling of the rest of the system to the indicated zone becomes stronger. (For a higher value of  $D_v$ , a stationary pattern may appear for lower values of the absorption parameter or in a larger system.)

In general, when this stationary regime does not occur, the oscillations are not inhibited. The system asymptotically reaches periodic, quasiperiodic, or chaotic inhomogeneous regimes. However, for large enough  $D_v$  (typically  $D_v > 2.3$ ), the system evolves toward a Turing pattern, that is also stationary, but of a completely different origin [10] than the stationary patterns described above. Turing patterns are generated by means of freezing fronts [11] which travel from  $x = L$  (the slower oscillating zone) to the rest of the system. As they advance, they inhibit the temporal oscillations

and leave behind the characteristic spatially-periodic structures. The process of formation of a Turing pattern is shown in Fig.1.

In Fig. 2 we show the phase diagram indicating the asymptotic behaviour of a system of length  $L = 70 \simeq 5\lambda_T$  with  $k_u = k_v \equiv k$  as function of  $D_v$  and  $k$ . The different regions correspond to Turing patterns (TP), inhomogeneous periodic oscillations (PO), inhomogeneous quasiperiodic oscillations (QP) and spatiotemporal chaos (CH).

In the periodic region (PO), the asymptotic behaviours correspond to regimes of periodic traveling waves from  $x = L$  (albedo bc) to  $x = 0$  (Neumann bc). The global period of the motion results always a little bit larger than  $\tau_0$ . This is because of the early slowdown of the oscillations occurring near  $x = L$ , that is later transmitted to the whole system. In Fig. 3 we show a spatiotemporal plot of the  $u$ -field corresponding to a time window of a typical asymptotic regime in the PO region.

To distinguish between PO, QP, and CH regimes we consider the succession  $\{t_n\}$  of times at which  $u(x = 0, t)$  reaches a local maximum as function of  $t$ , i.e. the times when

$$\frac{\partial}{\partial t}u(0, t)|_{t_n} = 0 \quad \text{and} \quad \frac{\partial^2}{\partial t^2}u(0, t)|_{t_n} < 0 \quad (4)$$

occur simultaneously. Then we define a new succession  $\{p_n = t_n - t_{n-1}\}$ .

The study of the behaviour of  $\{p_n\}$  provides a useful and simple way to determine the character of the dynamics (periodic, quasiperiodic or chaotic), as was already observed when dealing with inhomogeneous systems [9]. In the case of periodic motion the value of  $p_n$  converges to a constant  $p_\infty$  which coincides with the period of the global motion. In the case of quasiperiodic motion the  $p_n$ 's asymptotically show periodic or quasiperiodic behaviour. In the chaotic region the  $p_n$ 's exhibit highly disordered behaviour. Instead of considering the succession  $\{p_n\}$ , we work with the values of  $p_n$  plotted as a function of  $t_n$ . Hence we define a function of time  $p(t) \equiv p_n$  (strictly defined only for the discrete values  $t = t_n$ ). In Fig. 4 we show the typical plots of the  $p(t)$  for the PO, QP and CH regimes. In Fig. 4.a. the early time behaviour can be observed, in which the system at  $x = 0$  is performing the natural limit cycle oscillation of the medium, until the perturbation coming from  $x = L$  arrives slowing down the motion. It is worth here mentioning that we have not observed marginal profiles of  $p(t)$  where the determination of the kind of dynamics was not clear. However, in the transition zones between phases, the transients are long and it is necessary to observe the evolution for a very long time. Another remarkable fact is that disordered behaviour such as that appearing in Fig. 4.c. -here called chaotic- are chaotic in the sense of showing high sensitivity to initial conditions. We have verified this fact in a large number of cases by studying the evolution of the distance between solutions with different (but close) initial conditions, in the same way as it was done in [8].

In the asymptotic regimes of the QP and CH regions, it is not only waves traveling from  $x = L$  to  $x = 0$  that appear. There are intervals during which waves travel in the opposite sense, and also, from time to time, a center emitting waves in both directions may appear in any part of the system (specially in the CH regime). These effects are observed as defects and dislocations in the spatiotemporal plots of the  $u$ -fields. In the QP region, the defects appear periodically or quasiperiodically in time, while in the CH region they appear in a random way. In Fig. 5 we show a spatiotemporal plot corresponding to a chaotic regime, together with the plot of  $p(t)$  for the same time window. There, it can be observed that the arising of defects is related to the occurrence of maxima in  $p(t)$ , which indicates delays in the oscillations at  $x = 0$ .

In a small region of the transition zone between the PO and TP regions, which appears shadowed in the diagram of Fig. 2, the behaviour of the system is complicated. In general, a long chaotic transient appears that, later, eventually converges to Turing patterns, periodic or quasiperiodic behaviour. In this zone, the asymptotic behaviour is also possibly dependent on the initial condition -even when homogeneous and belonging to the indicated limit cycle. We have observed also Turing patterns that are generated by freezing fronts coming from  $x = 0$  (the Neumann bc) instead of from  $x = L$  (the albedo bc). One possible explanation for such peculiarities is that, in this zone of the diagram, the Turing instability is well established, but the albedo bc's introduce only a very small perturbation (because of the small values of  $ks$ ) that it is not always strong enough to excite the unstable spatial mode.

In the phase diagram of Fig. 2 we have indicated with dotted and dashed lines the zones where the transition between periodic and nonperiodic regimes respectively occur for a system with  $(k_u = 0, k_v \equiv k)$  and  $(k_u \equiv k, k_v = 0)$ . It can be seen that for  $(k_u = 0, k_v \equiv k)$  the transition occurs for similar -or even lower- values of  $k$  than in the case  $k_u = k_v = k$  but, for  $(k_u \equiv k, k_v = 0)$ , much larger values of  $k$  are needed in order to observe nonperiodic regimes. This indicates that the system is more sensitive to changes (or imperfections) in the boundary conditions of the  $v$ -field than of the  $u$ -field.

In the next section we analyze the dynamics of Eqs. (2) with partially absorptive bc's in two different bidimensional geometries.

### III. BIDIMENSIONAL SYSTEMS.

#### Circular system.

Firstly we consider the activator inhibitor model of Eqs.(2) in a circular system of radius  $R$  with albedo bc for both fields

$$\partial_r u(R) = -k_u u(R), \quad D_v \partial_r v(R) = -k_v v(R). \quad (5)$$

where  $r^2 = x^2 + y^2$  is the radial coordinate. We impose homogeneous initial conditions as in the previous section and study numerically the radial equations corresponding to (2):

$$\begin{aligned} \dot{u} &= \frac{1}{r} \frac{\partial}{\partial r} \left( r \frac{\partial u}{\partial r} \right) + f(u) - v \\ \dot{v} &= D_v \frac{1}{r} \frac{\partial}{\partial r} \left( r \frac{\partial v}{\partial r} \right) + u - \gamma v - c, \end{aligned} \quad (6)$$

with  $f(u)$ ,  $c$ ,  $\gamma$  and  $u_0$  as before. Analyzing the spatiotemporal plots  $(r, t)$  of the solutions and the  $p_n$ s (now defined at  $r = 0$ ), we have observed the same kinds of behaviour (periodic, quasiperiodic chaotic and Turing) as in the unidimensional system of the last section. In Fig. 6 we show the phase diagram for two different values of the radius of the system  $R$ .

In the first case, for  $R = 70$ , there is no CH phase because the system is not large enough to allow the required disorder on the dynamics of the oscillating phase in the different parts of the system to be produced. However, some chaotic isolated points have been observed in the shadowed zone in the transition to the TP region, where the properties of the dynamics are similar to those explained for the one-dimensional problem. For  $R = 80$  we have the same phases as in the unidimensional problem. Here, the asymptotic regimes correspond to target patterns, that are stationary in the TP region, and of waves traveling from  $r = R$  to  $r = 0$  in the PO region, and traveling in both directions in the QP and CH regions.

In the CH region, the radial symmetry is expected to be broken by small angular perturbations in real systems.

In both diagrams we show the transition lines from periodic to nonperiodic regimes for the cases ( $k_u \equiv k, k_v = 0$ ) and ( $k_u = 0, k_v \equiv k$ ). The observed shift of these lines relative respect to that for  $k_u = k_v = k$  are similar to those in the one dimensional problem. The conclusion that the system is more sensitive to boundary conditions on the  $v$ -field remains valid in bidimensional systems.

#### Band shaped system.

Now we consider Eqs.(2) in the same parameter region as before, in a long rectangular domain ( $0 \leq x \leq L_x, -L_y \leq y \leq L_y$ ) with  $L_y \ll L_x$  with different boundary conditions on its sides. We fix albedo bc at  $x = 0$  with  $k_u = k_v = 10$  (which means a strong absorption or very small reflectivity) and Neumann bc at  $x = L = 80$  ( $k_u = k_v = 0$ ). If we now fix Neumann bc also at the  $y = \pm L_y$  sides, we will have (for homogeneous initial conditions) an effective one-dimensional system equivalent to the one analyzed in section II. Instead, here we consider another albedo bc at  $y = \pm L_y$  with a different value of  $k \equiv k_u = k_v$ . In this case the patterns will not have translational symmetry in the  $y$ -direction. We fix  $D_v = 2$  and study numerically the solutions for different values of  $k$  and  $L_y$ . The situation to analyze is sketched in Fig. 7.

The one dimensional problem with  $k = 10$  at one end, and  $k = 0$  at the other is chaotic for  $L = 80, D_v = 2$ . Now, in the bidimensional system considered, it is expected that when increasing the albedo parameter on the  $y = \pm L_y$  sides from zero, the dynamics will begin to differ from the one of the one-dimensional system. In particular, if  $L_y$  is small and  $k$  large, we expect that the system will become stationary because of the stationary tendency introduced by this new boundary condition that will constrain the oscillations from the sides. This is in fact what simulations have shown. There are also intermediate values of  $k$  and  $L_y$  where the stationary tendency of the sides is not enough to completely inhibit the oscillations, but it is enough to change their characteristics from chaotic to quasiperiodic or periodic.

In Fig. 8 we show a diagram of the  $(k, L_y)$ -plane indicating the stationary and non-stationary regions as well as some points where periodic, quasiperiodic and chaotic dynamics have been observed.

It is posible to use a simple theoretical scheme in order to explain qualitatively the transition of the system from non stationary regimes to stationary ones when  $k$  is increased or  $L_y$  decreased. Such a scheme is based on a concept originated within the framework of nuclear reactor physics that simplifies noticeably the analysis of the so called

criticality problems or neutron density distributions, in many situations of interest. This is the concept of *geometrical buckling*. It helped to reduce the dimensionality of the problem, by assuming that directions transverse to the more relevant one can be essentially described by the fundamental mode. Such an assumption allows to include the effect of those extra dimensions through (lateral) "sink" contributions (that is taking into account the lateral leak) in a (typically one-dimensional) diffusion equation for the neutron density on the relevant direction [12]. For instance, using this approximation it is possible to estimate the critical mass or radius of a nuclear system. Clearly, such an approximation gives reliable results due to the linearity of the neutron diffusion equation (at least over time scales shorter than those at which the transport coefficients –cross section, diffusion constants– change).

Our system of equations is clearly nonlinear, hence such an approach could in principle not be applied. However, we qualitatively introduce such an idea forcing our equations to reduce their dimensionality and including associated sink or leak terms.

For the system in Eq.(2) in the rectangular geometry with  $L_y \ll L_x$ , and albedo conditions at  $y = \pm L_y$  given by

$$\partial_y u(x \pm L_y) = \mp k u(x, L_y), \quad D_v \partial_y v(x, \pm L_y) = \mp k v(x, L_y), \quad (7)$$

we will assume that the solution can be written as

$$\begin{aligned} u(x, y, t) &= \tilde{u}(x, t) \cos(q_u y) \\ v(x, y, t) &= \tilde{v}(x, t) \cos(q_v y). \end{aligned} \quad (8)$$

Hence, we are approximating the profiles of the distributions of  $u$  and  $v$  in the  $y$  coordinate as being independent of  $x$  and  $t$  except for a global factor. The cosine functions give a more or less desirable form for the densities, having a maxima at  $y = 0$ . Clearly, the ( $k = 0$ )–case corresponds to  $q_u = q_v = 0$  with solutions independent of  $y$ . We may expect that our approximation will give qualitatively better results for small  $k$ . From Eq. (7) we find the following relation that determines  $q_u$  and  $q_v$  as function of  $k, L_y$  and  $D_v$ :

$$k = q_u \tan(q_u L_y) \quad k = q_v D_v \tan(q_v L_y), \quad (9)$$

and from Eq.(2) we obtain

$$\begin{aligned} \dot{\tilde{u}} &= \frac{\partial \tilde{u}}{\partial x^2} - q_u^2 \tilde{u} + f(\tilde{u}) - \tilde{v} \\ \dot{\tilde{v}} &= \frac{\partial \tilde{v}}{\partial x^2} - D_v q_v^2 \tilde{v} + \tilde{u} - \gamma \tilde{v} - c. \end{aligned} \quad (10)$$

Now, since  $L_y \ll L_x$ , we might think that, whether the dynamics is stationary or not will depend only on  $k$  and  $L_y$  and not on what happens on the  $x$  coordinate [13], and we may consider the system as independent of  $x$ . We then obtain the following equations for a space independent activator–inhibitor system:

$$\begin{aligned} \dot{\tilde{u}} &= f(\tilde{u}) - q_u^2 \tilde{u} - \tilde{v} \\ \dot{\tilde{v}} &= \tilde{u} - D_v q_v^2 \tilde{v} - \gamma \tilde{v} - c. \end{aligned} \quad (11)$$

This system, for the chosen values of  $f(u)$ ,  $\gamma$ , and  $c$ , is oscillatory for null or small values of  $q_u$  and  $q_v$ , but there exist critical values of these quantities (which depend on  $L_y$ ,  $D_v$  and  $k$  through Eqs.(9)) beyond which the system begins to be monostable, i.e. asymptotically stationary. We associate this stationarity to that of our extended system. In Fig. 8 we have plotted with a dotted line the limit from stationary to non stationary regimes predicted in this way. Although the results do not agree quantitatively with those coming from simulations in the extended bidimensional system (solid line), the occurrence of the phenomenon is clearly well predicted qualitatively.

#### IV. FINAL REMARKS

We have analyzed the influence of partially absorptive boundary conditions in a typical reaction diffusion–model of an oscillatory active medium with different geometries. We have observed that the homogeneous periodic behaviour expected for the case of Neumann boundary conditions, when homogeneous initial condition are considered, is completely altered when the absorption parameter is increased from zero. For small absorption, the behaviour continues being periodic although the homogeneity is lost and traveling waves are observed. For higher absorption (with precise values of  $k$ 's depending on the diffusion constants), the periodicity is broken and quasiperiodic inhomogeneous oscillation and spatiotemporal chaos arise.

The kind of phenomena described here is expected to appear in real systems sharing the properties of the model. The predictions made for the three systems analyzed (one-dimensional, circular and band-shaped) illustrates what can be expected in more complicated situations. For example, let us consider the same dynamics given by Eqs. (2) with homogeneous initial conditions, but now in a square reactor with Neumann bc's everywhere except in a sector where albedo bc's are imposed. In Fig. 9 we show the contour plots of the  $u$ -fields for this system at several times taken in the asymptotic regime, assuming standard values of the parameters  $D_v$  and  $k$ . The spatiotemporal complexity arising is apparent.

When analyzing the transition lines from periodic to nonperiodic regimes for the cases ( $k_u \equiv k, k_v = 0$ ) and ( $k_u = 0, k_v \equiv k$ ) we have observed shifts of these lines relative to the case  $k_u = k_v = k$  that are similar in both the one dimensional and the circular cases. These results imply that the system is more sensitive to boundary conditions on the  $v$ -field than on the  $u$ -field.

As mentioned in the introduction, in a real experiment on oscillatory media, the waves emerging from the boundaries with imperfect reflectivity will interact with other patterns that may be spontaneously generated from fluctuations in the distribution of reactants in any part of the system. In this paper we have analyzed simpler situations that allowed us to isolate clearly the effects of the boundaries. The results obtained constitute a starting point for the study of more realistic situations.

**ACKNOWLEDGMENTS:** The authors thank V. Grunfeld for a revision of the manuscript. Partial support from CONICET (grant PIP Nro.4593/96), from Argentine, is also acknowledged.

- 
- [1] M.C. Cross and P.C.Hohenberg, Rev. Mod. Phys. **65**, 851 (1993); D. Walgraef, *Spatio-temporal pattern formation*, (Springer-Verlag, New York , 1997).
  - [2] E. Dulos, P. Davies, R. Rudovics and P. De Kepper, Physica D **98** 53 (1996).
  - [3] I. Sendiña-Nadal, V. Pérez-Muñuzuri, V. M. Eguíluz, E. Hernández-García and O. Piro, *Quasiperiodic patterns in boundary-modulated excitable waves*, Phys. Rev. Lett. submitted.
  - [4] V. M. Eguíluz, E. Hernández-García and O. Piro, Physica A **283** 48 (2000).
  - [5] J. J. Tyson and P. C. Fife, J. Chem. Phys. **73** N.5 2224 (1980).
  - [6] Lengyel I. and Epstein I. R., Proc. Natl. Acad. Sci. USA **89** 3977 (1992).
  - [7] A. Hagberg and E. Meron, Nonlinearity **7** 805 (1994).
  - [8] S. Bouzat and H.S. Wio, Phys. Lett. A **268** 323 (2000).
  - [9] S. Bouzat and H.S. Wio, *Pattern dynamics in bidimensional oscillatory media with bistable inhomogeneities*, Phys. Rev. E (in press).
  - [10] G. Nicolis, *Introduction to Nonlinear Science*, (Cambridge U.P., Cambridge, 1995).
  - [11] G. Heidemann, M. Bode and H.G. Purwins, Phys. Lett. A **177** 225 (1993).
  - [12] P.F. Zweifel, *Reactor Physics*, McGraw-Hill, NY (1973), chp.3; K.H Beckurts and K. Wirtz, *Neutro Physics*, (Springer-Verlag, Berlin 1964), chp.9.
  - [13] The analysis of the dynamics of the  $x$  coordinate would determine, in case the motion is not stationary, whether it is periodic, quasiperiodic, or chaotic; but this is an aspect in which we are not interested here.

FIG. 1. Propagation of a freezing front leading to the formation of a Turing pattern. Spatiotemporal plot of the  $u$ -field for  $L = 70$ ,  $D_v = 2.4$  and  $k_u = k_v = 1$ .

FIG. 2. Phase diagram ( $(D_v, k)$ -plane) indicating the asymptotic behaviour of the one dimensional system for  $L = 70$  and  $k_u = k_v \equiv k$ . The regions corresponding to inhomogeneous periodic oscillations, Turing patterns and quasiperiodic and chaotic behaviour, are indicated with PO, TP, QP, CH respectively. The transitions from periodic to nonperiodic regimes in the cases ( $k_u \equiv k, k_v = 0$ ) and ( $k_u = 0, k_v \equiv k$ ) are indicated respectively with dashed and dotted lines.

FIG. 3. Spatiotemporal plots of the  $u$ -fields in the asymptotic regime of the PO region. Calculations for  $D_v = 1.8, k_u = k_v = .02$ .

FIG. 4. Typical plots of  $p(t)$  in for: (a) PO region ( $D_v = 1.8, k_u = k_v = .02$ ); (b) QP region ( $D_v = 1., k_u = k_v = 1.$ ); (c) CH region ( $D_v = 1.8, k_u = k_v = 1.$ ).

FIG. 5. Dynamics in the CH region. Top: spatiotemporal plot of the  $u$ -field for  $D_v = 1.8, k_u = k_v = 1$  in a temporal window of the asymptotic regime. Bottom: plot of  $p(t)$  for the same system in the same time window.

FIG. 6. Phase diagrams indicating the asymptotic regimes of circular systems for: (a)  $L = 70$ ; (b)  $L = 80$ . In both cases, the regions are indicated with the same nomenclature as in figure 2. With dashed and dotted lines we indicate the transitions from periodic to nonperiodic regimes in the cases ( $k_u \equiv k, k_v = 0$ ) and ( $k_u = 0, k_v \equiv k$ ) respectively.

FIG. 7. Sketch of the band shaped system indicating the different boundary condition considered.

FIG. 8. Diagram indicating the different behaviours observed in the band shaped system as function of  $k$  and  $L_y$ . The solid line indicates the transition between stationary and nonstationary regimes calculated from simulations. The dotted line corresponds to the estimation of this frontier with the discussed theoretical arguments. Crosses, squares, circles and triangles correspond to the observations in simulations of stationary, periodic, quasiperiodic and chaotic behaviour respectively.

FIG. 9. Contour plots of the  $u$ -fields for a square system with Neumann bc's except in the right bottom corner (indicated with arrows in the left figure) where we have fixed albedo bc's with  $k_u = k_v = 1$ . From left to right the plots correspond to times  $t = 2000, 2004, 2008, 2012$  and  $2016$ . The other parameters are  $D_v = 2$ , and  $L_x = L_y = 60$ .

FIG 1. Bouzat and Wio.

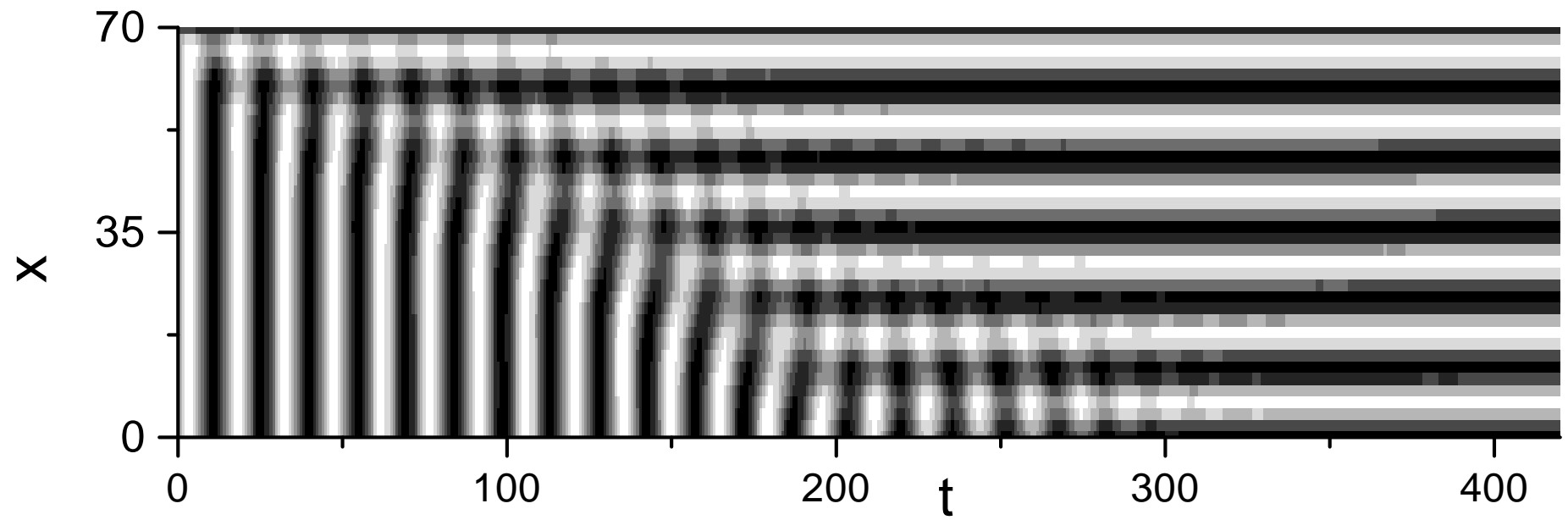




Fig 2. Bouzat and Wio.

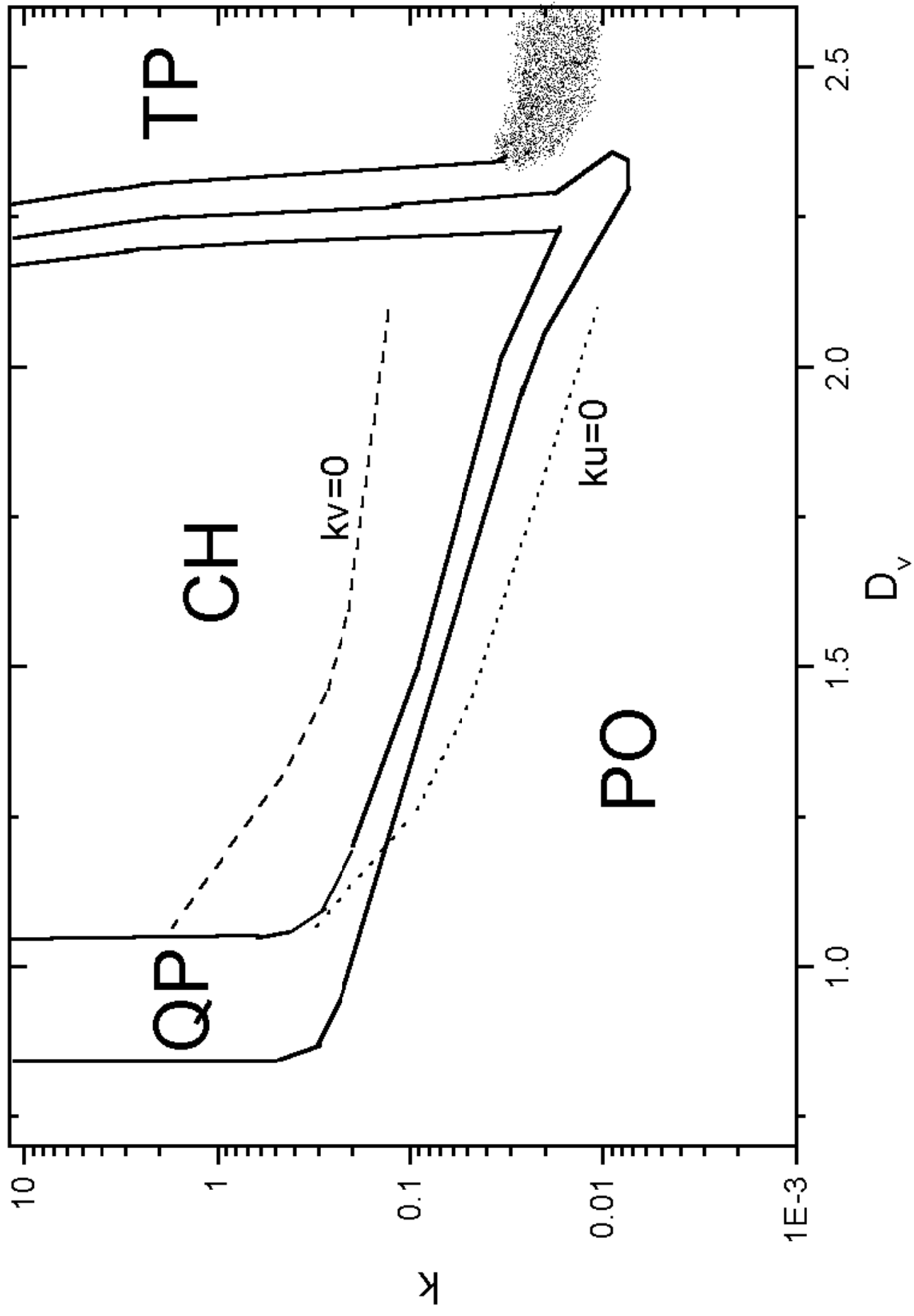
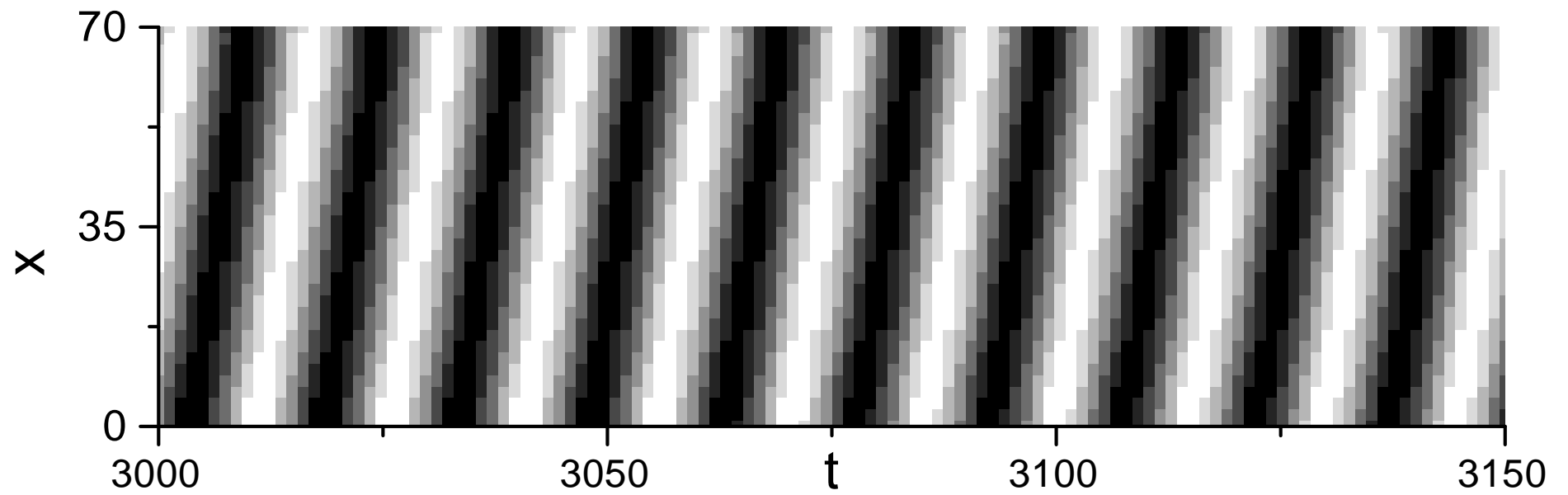


FIG 3. Bouzat and Wio.



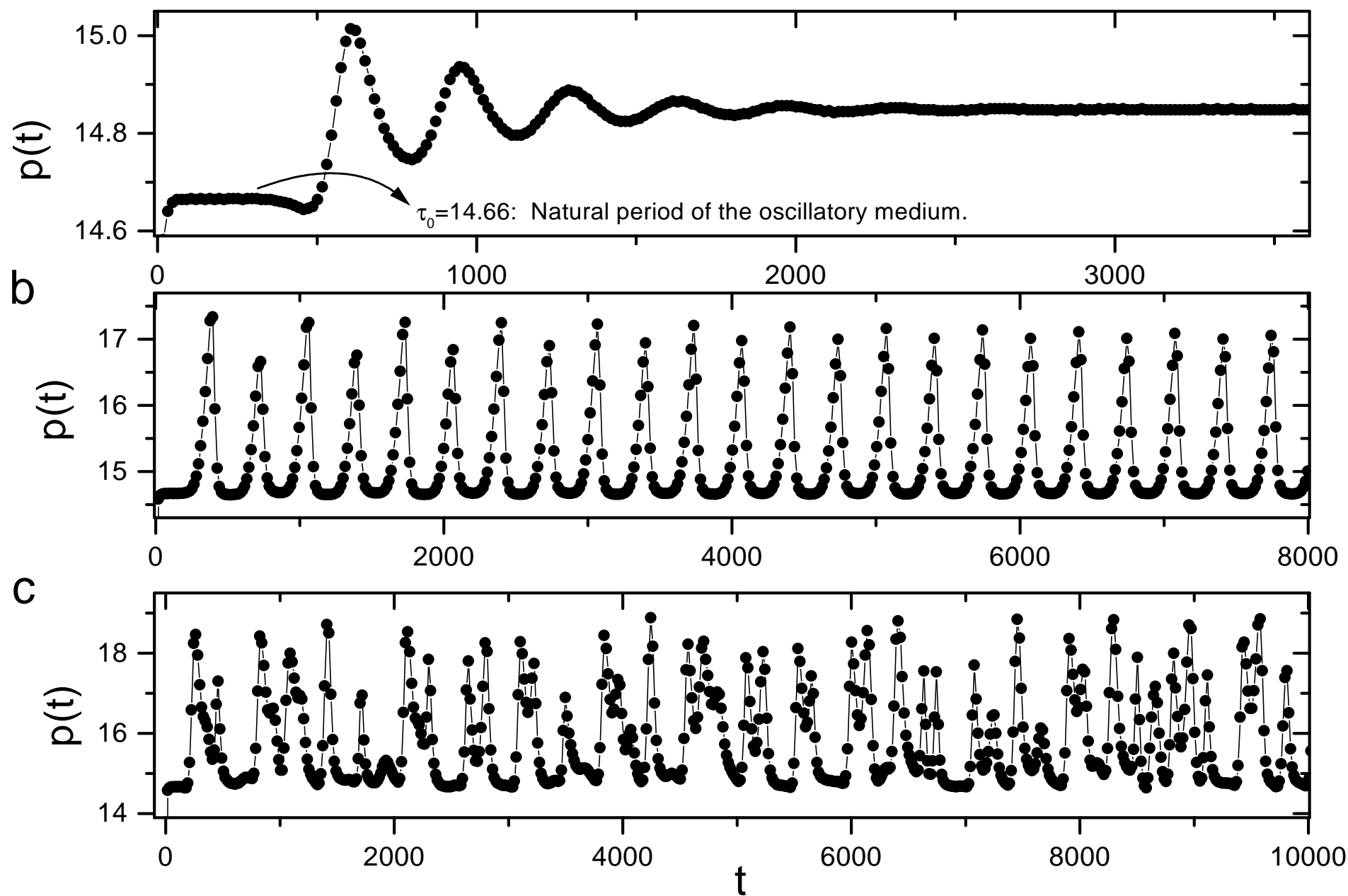
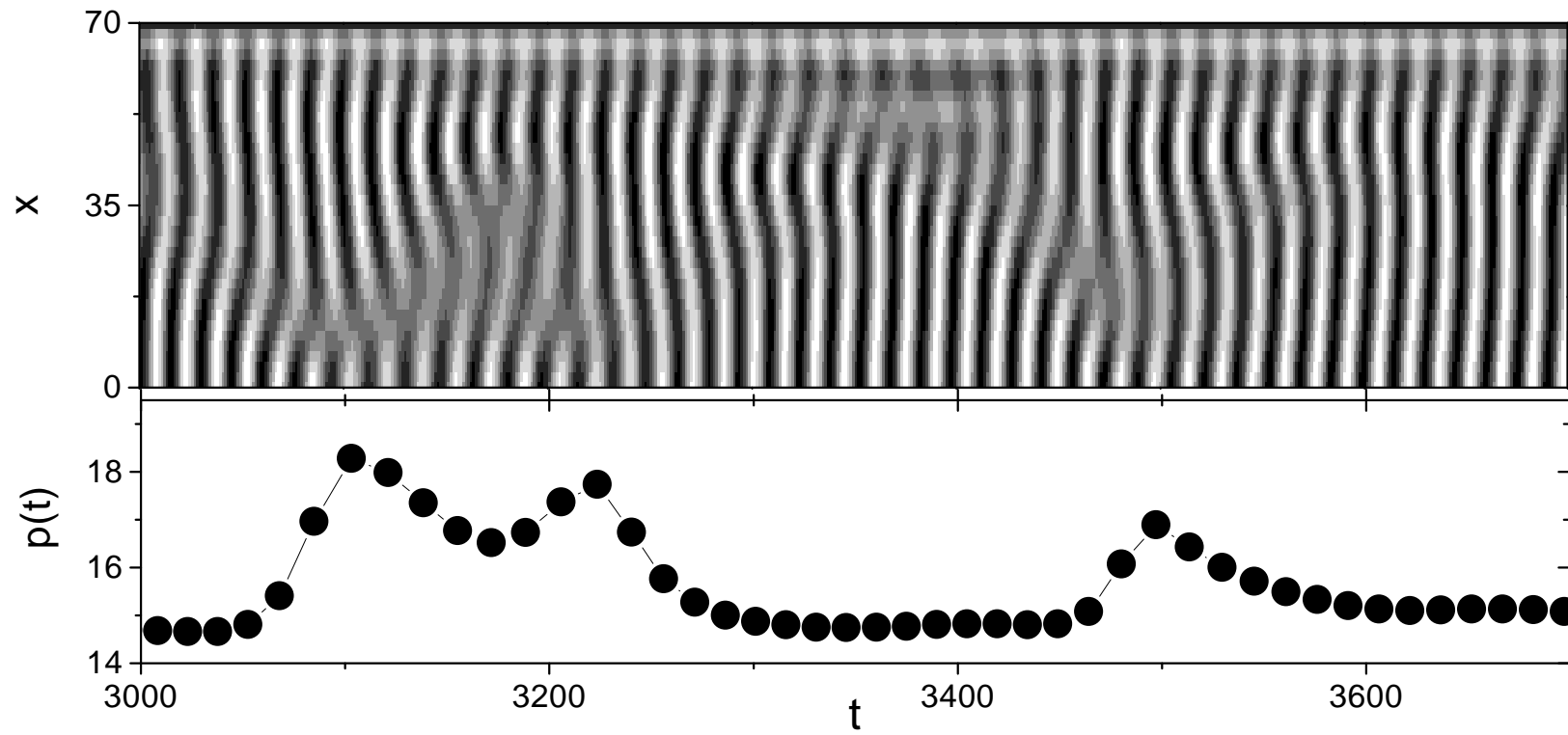
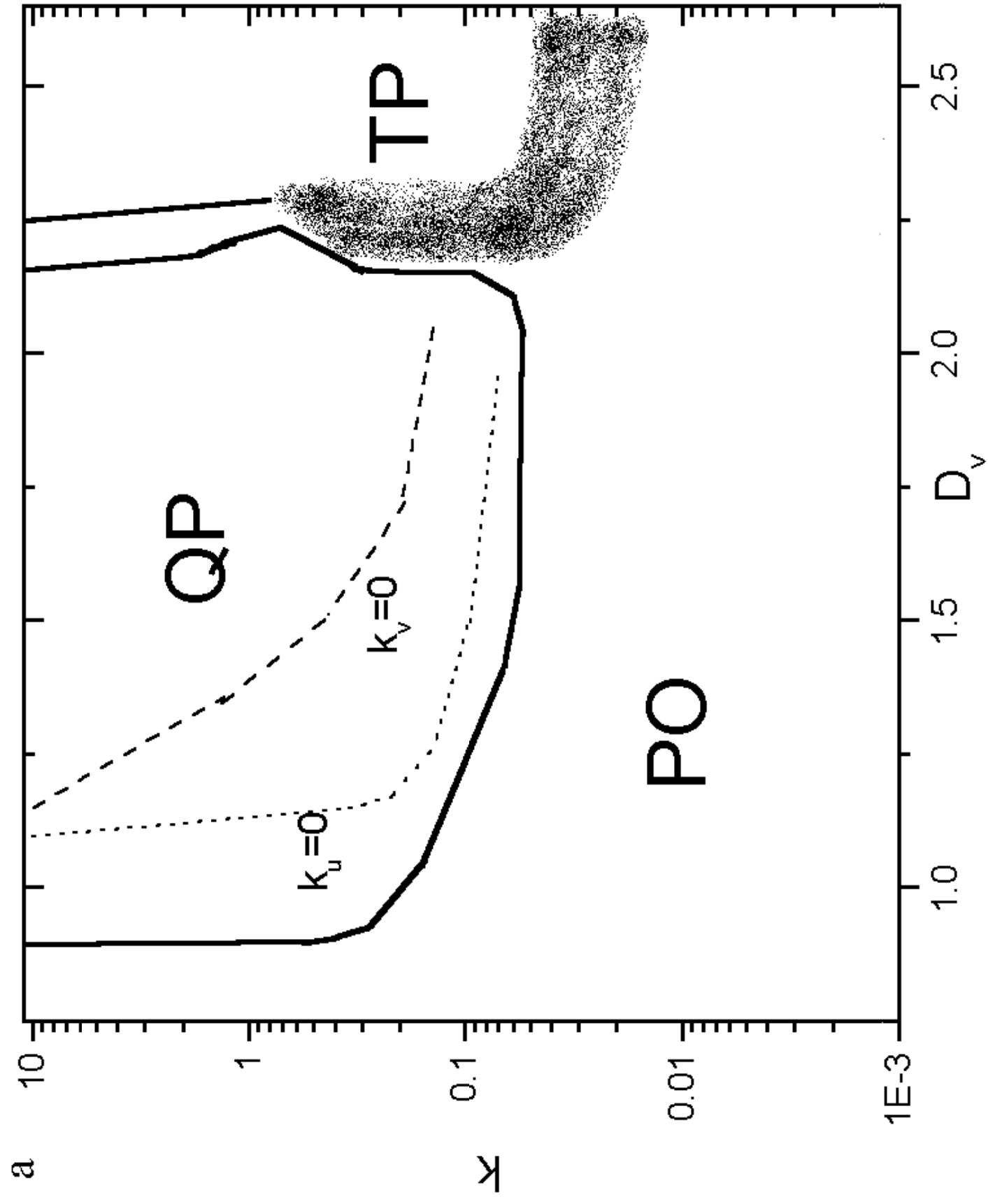
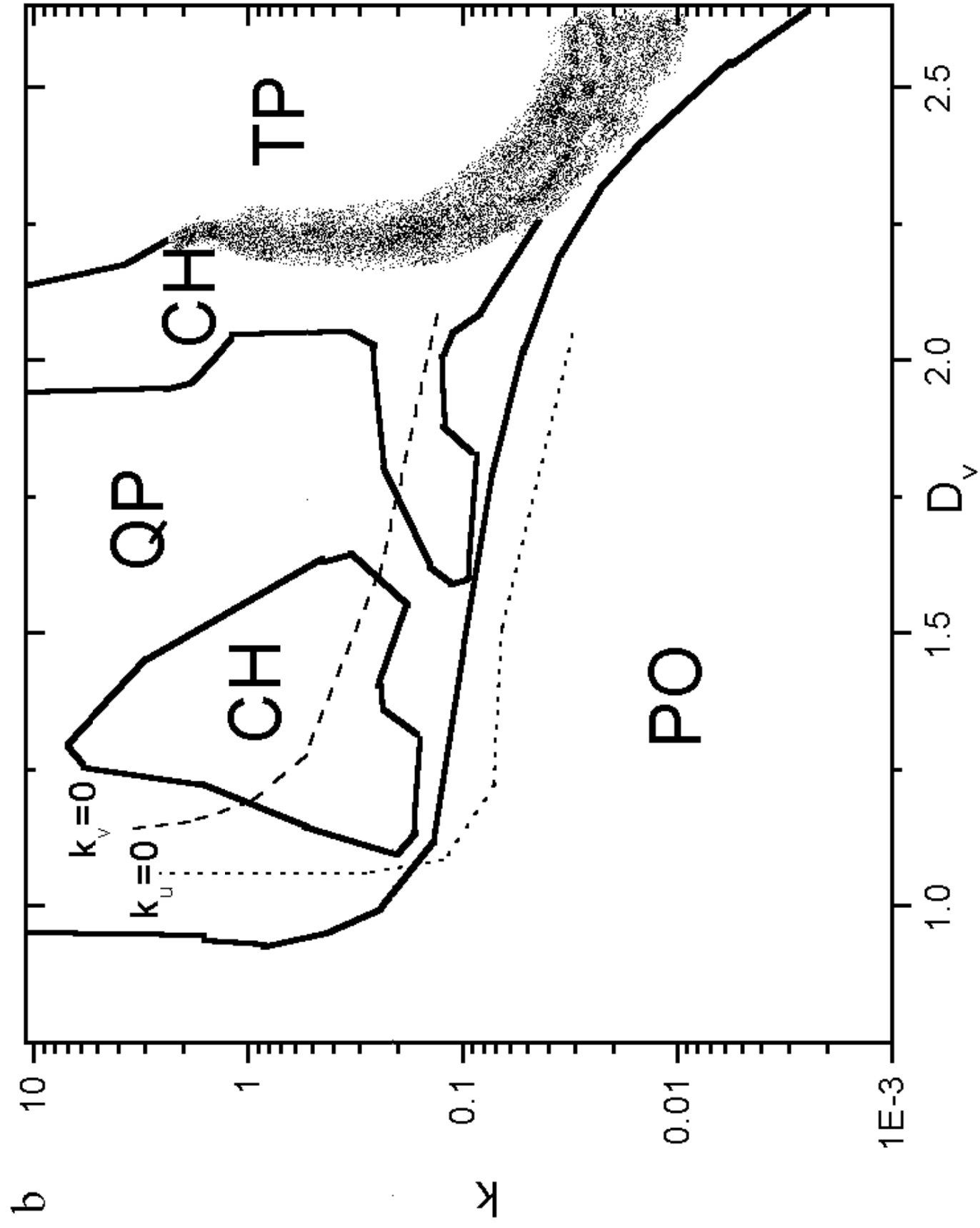


FIG 4. Bouzat and Wio.

Fig 5. Bouzat & Wio.



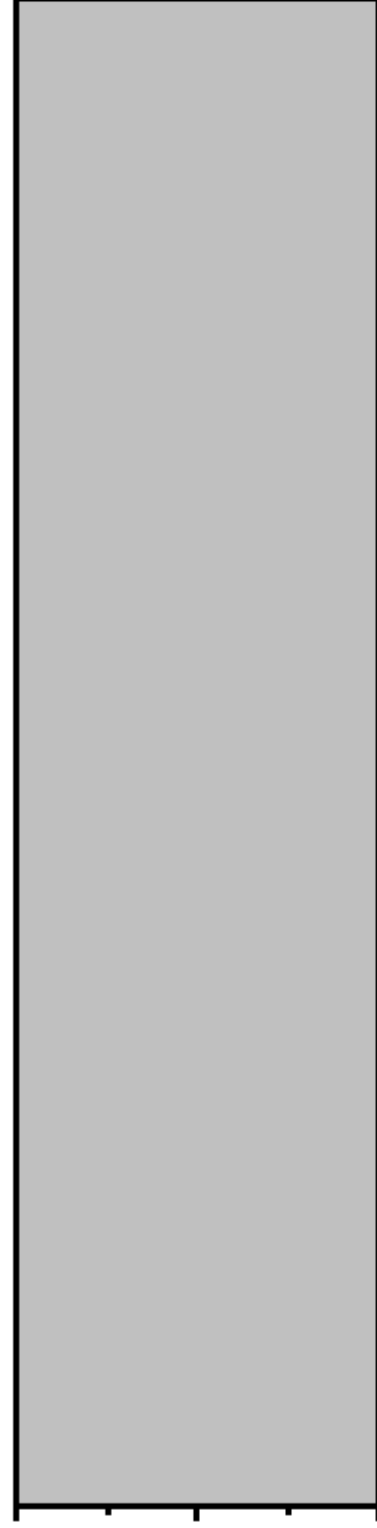




Albedo 2 :  $k_u = k_v = k$

$2 L_v$

Albedo 1  
 $k_u = k_v = 10$



Neumann

Albedo 2 :  $k_u = k_v = k$

$L_x$

